Published in final edited form as:
Neuron. 2007 May 24; 54(4): 547–557. doi:10.1016/j.neuron.2007.04.029.

Zfp423/OAZ participates in a developmental switch during olfactory neurogenesis

Li E. Cheng and **Randall R. Reed**
Center for Sensory Biology, Department of Molecular Biology and Genetics, Department of Neuroscience, Johns Hopkins University School of Medicine, 725 N Wolfe St, Baltimore, MD 21205

Summary

The coordination of gene expression is critical for cell differentiation and the subsequent establishment of tissue function. We show here that a multiple zinc-finger transcription factor, *zfp423/OAZ*, is transiently expressed in newly differentiating olfactory receptor neurons (ORNs) and has a key role in coordinating the expression of immature and mature stage-specific genes. OAZ deletion in mice impairs aspects of ORN differentiation, particularly the patterns of axonal projection to the olfactory bulb. OAZ gain-of-function experiments show that sustained OAZ expression throughout ORN maturation arrests ORN development at an immature stage and alters OR gene expression. Importantly, reintroducing OAZ expression in mature ORNs suppresses mature marker expression and reactivates immature-specific markers. Together, theses experiments suggest that OAZ participates in a developmental switch regulating the transition from differentiation to maturation in ORNs.

Introduction

The olfactory receptor neurons (ORNs) are continuously generated from a population of neuroblast-like stem/progenitor cells located at the basal olfactory epithelium (OE). This lifelong olfactory neurogenesis is under the control of a temporal series of intrinsic transcriptional cascades (Nicolay et al., 2006), some of which are regulated by extrinsic cues (Kawauchi et al., 2004; Kawauchi et al., 2005; Wu et al., 2003). During ORN development, olfactory stem cells undergo infrequent asymmetric cell divisions to generate transient amplifying progenitors (*Mash1*-positive) and subsequently, *Ngn1*-positive immediate neuronal precursors (Calof et al., 2002; Cau et al., 2002). The division of *Ngn1*-positive cells generates daughter cells that differentiate into ORNs and express characteristic markers including neural cell adhesion molecule (NCAM), olfactory maker protein (OMP) and olfactory-specific genes essential for odorant transduction (Bakalyar and Reed, 1990; Brunet et al., 1996; Calof and Chikaraishi, 1989; Jones and Reed, 1989; Kawauchi et al., 2004).

Extrinsic signaling molecules implicated in olfactory neurogenesis include the fibroblast growth factor (FGF) and transforming growth factor-β (TGF-β) superfamilies (Kawauchi et al., 2004; Kawauchi et al., 2005). These signaling molecules, particular the bone morphogenic proteins (BMPs) exert both positive and negative effects on ORN neurogenesis, depending on the type of the signaling molecule, the concentration and the stage at which they act (Kawauchi et al., 2004; Shou et al., 1999; Shou et al., 2000; Wu et al., 2003). Despite considerable progress

in defining transcription factors and signaling molecules in OE neurogenesis, much less is known about the key transcriptional regulators mediating the interaction between these two aspects of regulation.

The *Zfp423*/*OAZ* protein, containing 30 kruppel-like C_2H_2 zinc-fingers is an attractive candidate to mediate extrinsic regulation of the transcriptional cascade. OAZ (*O*/*E* associated zinc-finger protein) was identified as an inhibitor of O/E proteins, a family of transcriptional factors involved in terminal ORN differentiation (Wang and Reed, 1993; Wang et al., 1993; Wang et al., 1997). OAZ binds to O/E proteins using a subset of zinc-finger domains and abolishes O/E binding to consensus binding sites present in olfactory-specific promoters (Tsai and Reed, 1997; Tsai and Reed, 1998). This negative regulation of O/E activity was proposed to prevent premature differentiation of immature ORNs. Independently, OAZ was also identified as a cofactor of Smad proteins in the BMP-signaling pathway (Hata et al., 2000; Ku et al., 2006; Shim et al., 2002). The zinc-finger domains mediating Smad interaction are distinct from those that engage in O/E proteins (Hata et al., 2000). The presence of BMPs and their receptors in the olfactory system and the proposed role of BMPs in regulation of ORN differentiation (Dewulf et al., 1995; Wu et al., 2003; Zhang et al., 1998) suggest that OAZ might have an important role in integrating BMP signaling and O/E activity at critical stages of ORN differentiation.

In this study, we provide *in vivo* evidence that OAZ regulates the transition from differentiation to maturation in ORNs. OAZ is transiently expressed in newly generated postmitotic ORNs. OAZ deletion in mice impairs ORN differentiation. Importantly, reintroducing OAZ into mature cells is sufficient to revert mature cells to an immature phenotype. These arrested, immature cells accumulate in OE and are perturbed in normal olfactory receptor (OR) gene selection and expression.

Results

OAZ expression is downstream of *Mash1* and partly overlaps with *Ngn1*+ *cells*

To elucidate the pattern of OAZ expression in OE, we initially utilized an *OAZ-lacZ* reporter mouse line (OAZ^{lacZ}, XB409), derived from a gene-trap screen in ES cells (Stryke et al., 2003). This line contains a β-geo gene-trap vector insertion into the last intron of *OAZ* gene, resulting in a deletion of nine amino acids from the OAZ C-terminus and expression of an OAZ-lacZ fusion protein. X-gal staining in $OAZ^{lacZ/+}$ mice at E18 revealed a broad OAZ expression in the developing OE (Figure 1A). The expression decreased postnatally and was restricted to the basal OE (Figure 1B, C), the site of continuous olfactory neurogenesis in adults.

During ORN development, progenitors express the molecular markers *Mash1* and *Ngn1* at successive stages and migrate apically in the OE (Calof et al., 2002; Cau et al., 2002). To identify the stage at which *OAZ* is expressed, we introduced $Mash1^{GFP/+}$ and $Ngn1^{GFP/+}$ reporter knock-in mice, in which a nuclear GFP reporter precisely replaces the respective coding regions and faithfully mimic expression of the endogenous gene (Leung and Reed, unpublished). In $OAZ^{lacZ/+}Mash1^{GFP/+}$ mice, *OAZ*-expressing cells were identified with X-gal staining (Figure 1D) and *Mash1*-expressing cells were labeled with an anti-GFP antibody (Figure 1E). OAZ-expressing cells were located apically to *Mash1*-expressing cells (Figure 1F), and were essentially absent in E18 *Mash1*-null mice (Figure 1J), suggesting that *OAZ* is downstream of *Mash1*. In $OAZ^{lacZ/+}Ngn1^{GFP/+}$ mice, *Ngn1* and *OAZ*-expressing cells were largely located in the same layer (Figures 1G–I). In cofocal images, *Ngn1*/*OAZ* double-labeled cells were predominantly located between the more basal *Ngn1*-expressing cells and more apical *OAZ*-expressing cells (Figure 1K), suggesting that *OAZ* expression may be initiated as cells ceased *Ngn1* expression. Furthermore, OAZ was confined to postmitotic cells when

examined by BrdU labeling (Figure 1L). Together, these observations indicate that *OAZ* is expressed in newly differentiating ORNs.

Mature cells are reduced in *OAZ*$^{-/-}$ mice

In parallel, we generated a reporter-tagged *OAZ*-null allele by targeted deletion of the *OAZ* large exon 4 and insertion of *IRES-YFP*-polyA. This presumptive functional null allele lacks 1180/1292 amino acids of the native OAZ protein including all the known DNA-binding and protein-binding domains and is hereafter referred to as *OAZ*$^{-}$. Homozygous *OAZ*$^{-/-}$ mice exhibited profound cerebellar defects and died by approximately four weeks. The cerebellar phenotype of other *OAZ* alleles has been described elsewhere (Alcaraz et al., 2006; Cheng and Reed, 2007; Warming et al., 2006). The olfactory turbinates of *OAZ*$^{-/-}$ mice display normal organization with a slightly smaller nasal cavity and correspondingly reduced OE area. To examine subsequent stages of ORN development, OE sections (PD 20–25) were examined with the ORN lineage marker O/E, mature ORN marker OMP, and differentiation markers GAP43 and NeuroD1. The pattern of O/E immunostaining in the epithelium from wild-type and *OAZ*$^{-/-}$ mice were indistinguishable (Figure 2A). However, the number of mature cells visualized by OMP immunostaining was fewer in P20 *OAZ*$^{-/-}$ mice (data not shown) and, when quantified by *in situ* hybridization (Figure 2B), was reduced 30% (wt, 890±30/mm; *OAZ*$^{-/-}$, 635±15/mm, Figure 2F). In contrast, there were no changes in the expression of GAP43 (Figure 2C) and NeuroD1 (Figure S1C in supplemental data). It is noteworthy that *Evi3*, an *OAZ* homolog gene that also interacts with O/E protein (Hentges et al., 2005; Warming et al., 2003), is present at low levels in the OE and displays a pattern of expression similar to OAZ (Figure S2), which may obscure a complete analysis of loss-of-function of OAZ in the OE.

The reduction of mature cells could arise from decreased proliferation of progenitors, delayed maturation, and/or reduction of cell lifespan. No significant changes in the number of BrdU-positive cells were observed between wild-type and *OAZ*$^{-/-}$ mice examined at P2, P7 and P20 (Figure 2D, G). TUNEL staining, however, showed a twofold increase in the number of apoptotic cells in *OAZ*$^{-/-}$ mice (wt, 7.0±1.9/mm; *OAZ*$^{-/-}$, 17.6±10.0/mm, Figure 2E, H) that could account for the decease in mature neurons, but additional effects of *OAZ* on progression of maturation are possible. The observed OE phenotype was consistent along the anterior to posterior axis and across different dorsal-ventral zones in the OE (Figures S1A, B).

Olfactory axonal projection is impaired in *OAZ*$^{-/-}$ mice

A hallmark of ORN organization is that cells expressing a particular OR gene project their axons to spatially defined glomeruli in the olfactory bulb (OB) (Vassar et al., 1994). The OB in *OAZ*$^{-/-}$ mice was smaller, a phenotype also observed in other genetic models where primary ORN afferents fail to project or lack odor-evoked activity (Baker et al., 1999; Hirata et al., 2006). We examined ORN projection by introducing the *O/E3-tauGFP* reporter (Wang et al., 2004). In whole-mount view, ORN axons failed to innervate the dorsal caudal region of the OB in *OAZ*$^{-/-}$ mice (Figure 3B and Figures S3B–D). In coronal sections, the caudal dorsal OB was essentially devoid of olfactory nerves and glomeruli; instead, additional glomeruli were concentrated on the ventral surface (Figures S3K–M). A similar OB phenotype was observed when projection were visualized with an *OMP-taulacZ* reporter (Mombaerts et al., 1996) (Figures 3C, D).

We examined the laminar organization of the OB using makers for OB neurons and olfactory axons. In neonatal and adult mice, GAP43 mRNA is detected in mitral cells and periglomerular cells (Verhaagen et al., 1990) (Figure 3E–H). In *OAZ*$^{-/-}$ mice, the dorsal OB surface was devoid of periglomerular cells and the mitral cell layer was pushed inwardly by the ventrally accumulated glomeruli (Figure 3F, H). Consistently, when olfactory axons were labeled with

OMP (Figures 3I–L), the dorsal OB surface lacked an olfactory nerve layer (ONL), but a fibrocellular mass-like structure composed of tangled axons and disorganized glomeruli was observed at the ventral surface (Figure 3L).

We next examined the projection of individual ORNs by introducing reporter-tagged OR alleles (Mombaerts et al., 1996; Zheng et al., 2000). In contrast to two topographically fixed M72 glomeruli in wild-type mice (arrows in Figure 3M, N), multiple M72 projection sites were detected (10/12 OBs), or only wandering axons could be observed (2/12 OBs) in $OAZ^{-/-}$ mice. Interestingly, a subset of M72 neurons projected to a glomerulus located in a similar position as in *OAZ* wild-type mice (arrows in Figure 3O–R), whereas the remaining majority axons projected to multiple, more ventral glomeruli (arrowheads). The disrupted projection pattern was also observed for the M71-expressing cells using the *M71-IRES-TauGFP* reporter (control, n=8 mice, $OAZ^{-/-}$, n=12 mice). ORNs expressing the P2 OR extend much shorter axons and project to a ventral region of the bulb. In $OAZ^{-/-}$ mice, the P2 axons innervate glomeruli that were anteriorly shifted and wandering axons were observed at higher frequency (data not shown).

Gain-of-function: targeted-*OAZ* expression throughout ORN development

The loss-of-function experiments described above suggest that OAZ is important for the normal program of ORN differentiation, particularly the projection of olfactory axons. The proposed role of *OAZ* as an inhibitor of O/E transcription factor function (but not O/E protein expression) led us to ask whether sustained *OAZ* expression was sufficient to arrest ORN development. We designed a dominant gain-of-function knock-in allele that expresses OAZ from the *O/E3* locus (Figure 4A). The *O/E3* promoter would drive sustained OAZ expression throughout ORN development. An IRES-driven YFP reporter was included to facilitate identification of the *O/E3-OAZ* expressing cells.

The *LTNL* cassette used for ES cell selection affects gene expression from the *O/E3* promoter. In the initial $O/E3^{OAZ\text{-}LTNL}$ mouse line that still carries *LTNL*, no YFP expression was detected in the OE. However, after CRE-mediated removal of *LTNL*, heterozygous $O/E3^{OAZ/+}$ mice could be readily distinguished by their small size and YFP expression (mean weight at P21: wt, 11.1±0.6g, n=7; $O/E3^{OAZ/+}$, 7.5±0.8g, n=7, P<0.001). We speculate that *LTNL* blocks a downstream enhancer of the *O/E3* promoter, resulting in the absence of *OAZ-YFP* expression in cassette-containing mice. A similar phenomenon is seen with other insertions at this locus (unpublished data). Since both the $O/E3^{OAZ\text{-}LTNL}$ mice and $O/E3^{OAZ/+}$ mice contain one deleted copy of the *O/E3* gene, analysis of $O/E3^{OAZ\text{-}LTNL}$ mice (which display a wild-type phenotype) provides strong evidence that the phenotype we observed in $O/E3^{OAZ/+}$ mice results from expression of *OAZ*, rather than simply the loss of one copy of *O/E3*. This special feature also provides for conditional control of OAZ-YFP expression.

Sustained *OAZ* expression arrests ORN maturation

We characterized ORN development in $O/E3^{OAZ/+}$ mice using mature markers OMP and Adenylyl cyclase 3 (AC3), the general neuronal marker NCAM, and the immature marker GAP43. In $O/E3^{OAZ/+}$ mice, there was a dramatic reduction in the number of mature ORNs visualized by OMP (Figures 4B, C) and AC3 immunostaining (Figures 4F, G). Intriguingly, there was no overlap between expression of OAZ and the mature cell markers; cells that displayed high levels of OMP or AC3 expression were those that failed to express the *OAZ*-linked YFP reporter (arrows in Figures 4C–E and G–I). Furthermore, the YFP-positive cells in $O/E3^{OAZ/+}$ mice expressed NCAM, indicative of a normal neuronal lineage (Figures 4J–M). *In situ* hybridization revealed that the majority of cells in the epithelium of $O/E3^{OAZ/+}$ mice were positive for GAP43 (Figures 5C, D, n=6 mice), indicating that the cells were arrested at an immature stage. In contrast, GAP43 expression was restricted to the basal immature cell

layer in cassette-containing, phenotypically wild-type mice (Figures 5A, B). Importantly, the number of GAP43 positive cells in *O/E3*$^{OAZ/+}$ mice was markedly increased in comparison to wild-type OE.

The reduction of mature cells was also confirmed by using an OMP-taulacZ reporter (Figures 6A–D). There was a 95% reduction of OMP-positive cells in *O/E3*$^{OAZ/+}$ mice compared with OMP *in situ* hybridization of wild-type mice (wt, 865±66/mm; *O/E3*$^{OAZ/+}$, 47±28/mm, Figure 6E). In parallel, *in situ* hybridization with several OR gene probes revealed that OR genes were not expressed at high levels in these immature cells (Figure S4). If these cells are blocked from completing the normal differentiation program by the persistent expression of *OAZ*, one might expect an increase in apoptosis. We observed an 8-fold increase in TUNEL-positive cells in *O/E3*$^{OAZ/+}$ mice (Figures 6F, G and H, wt, 9.4±5.4/mm; *O/E3*$^{OAZ/+}$, 76.5±25.2/mm). However, these apoptotic cells still represent only a small fraction of the total immature population in the epithelium. Taken together, these experiments indicate that ORN maturation is arrested at an immature neuronal stage and accumulate in greater numbers in*O/E3*$^{OAZ/+}$ mice.

OAZ expression is sufficient for an immature ORN phenotype

The *OAZ*-mediated arrest of ORN maturation is consistent with its ability to block O/E-mediated expression from reporter constructs in heterologous cell lines (Tsai and Reed, 1997). We next asked whether OAZ expression is sufficient for an immature phenotype by utilizing the gain-of-function *O/E3*$^{OAZ\text{-}LNL/+}$ allele to reintroduce *OAZ* expression in mature ORNs. Specifically, *O/E3*$^{OAZ\text{-}LNL/+}$ mice were crossed with mice in which the CRE recombinase is under the control of the *OMP* promoter (*OMP-CRE)* (Li et al., 2004). As expected, *LTNL* cassette removal led to appearance of *OAZ-YFP* in the mature neuronal layer (Figure 5I). In these mice, GAP43 *in situ* hybridization revealed a second population of GAP43-expressing cells present in the apical region (Figures 5E, F, n=4) in addition to the basal layer of the endogenous GAP43-expressing cells. This pattern contrasts with the basally-restricted GAP43-positive cells observed in the *O/E3*$^{OAZ\text{-}LNL/+}$ mice (Figure 5B). Subsequent OMP/GAP43 double-labeling revealed that OMP expression was suppressed in these reactivated GAP43-positive cells (Figures 5G, H). Messenger RNA for ORs and other mature ORN markers examined by *in situ* hybridization were also reduced (data not shown). Together, these experiments indicate that *OAZ* expression is sufficient to establish an immature ORN phenotype.

Altered axonal projection and OR gene expression in *O/E3*$^{OAZ/+}$ mice

We further characterized the OAZ-mediated arrest of ORN maturation and examined ORN projection using the OMP-tauLacZ reporter. In *O/E3*$^{OAZ/+}$ mice, the dorsal OB surface was largely devoid of glomeruli; the few projecting axons reaching the dorsal surface migrated along aberrant paths instead of converging (Figures 7A, B). Coronal sections confirmed the lack of an extensive ONL and glomerular layer at the dorsal and lateral OB surface, while some glomeruli remained at the medial surface (Figures 7C–F). Further analysis showed that even though GAP43-expressing immature cells could initiate their axonal growth in *O/E3*$^{OAZ/+}$ mice (Figures 7G, H), the majority failed to innervate the bulb (Figure S5). The medial OB surface contained OMP-positive axons and disorganized glomerular structures, but the lateral surface contained only a thin ONL (Figures 7I–K) that presumable derive from the “escaper” cells. The expression of tyrosine hydroxylase, a marker for periglomerular interneurons, was also reduced at the lateral OB surface consistent with the reduced innervation by ORN axons (Figures 7L–N).

We next examined OR-dependent axonal convergence. In *O/E3*$^{OAZ/+}$ mice, the projections from both P2 and M72-expressing cells to the OB were greatly reduced. The remaining P2 and

M72 projecting axons were unable to converge but spread along the medial surface of the bulb (Figures 8A, B and Figure S6).

Interestingly, whole-mount X-gal staining of taulacZ-tagged M72 receptor revealed a large number of weakly stained cells in the epithelium (arrows in Figure 8D). In coronal sections, these weakly stained cells displayed short dendrites and no obvious axon extensions although the faint signal might prevent visualization of these structures. (Figure 8F). Confocal imaging revealed that most of these cells (94%, n=89) were also expressing OAZ-YFP. The level of M72 gene expression in these immature cells, inferred by the intensity of X-gal staining, was much lower than that observed for axon-projecting M72 cells in wild-type mice (arrowheads in Figure 8E) and could not be detected by *in situ* hybridization (Figure S4). Remarkably, the total number of M72-taulacZ expressing cells was three-fold greater in the epithelium of *O/E3*$^{OAZ/+}$ mice than in control littermates (wt, 1.2±0.3/mm, n=3; *O/E3*$^{OAZ/+}$, 4.7±0.7/mm, n=3, P<0.002, Figure 8G). The OAZ-mediated arrest of ORN maturation appears to perturb OR expression and alters the number of cells that have chosen a particular receptor for expression.

Discussion

OAZ mediates the transition from differentiation to maturation in ORNs

First identified as a transcriptional partner of O/E proteins, OAZ was also found to mediate BMP-signaling pathways through independent domains of the protein. The loss-of-function and gain-of function experiments described here suggest that in ORN development, OAZ may coordinately regulate the duration of immature gene expression and the onset of mature gene expression (Figure S7). These two developmental processes may arise through distinct O/E and BMP-mediated pathways.

In the OE, OAZ is transiently expressed in newly generated differentiating ORNs. Consistent with its postmitotic expression, OAZ deletion does not affect proliferation of olfactory progenitors. Instead, we observed decreased mature cells, impaired axonal targeting and increased apoptosis in *OAZ*$^{-/-}$ mice. Similar but less severe axonal targeting defects were also observed in *O/E2* and *O/E3*-null mice (Wang et al., 2004). Therefore, the O/E-OAZ interaction may regulate (directly or indirectly) ORN axonal growth and/or targeting. The overlapping expression of Evi3 and OAZ in the OE may moderate the phenotype in the loss-of-function *OAZ*-null mice and obscure a critical role for OAZ in the transition from immature to mature ORNs. However, the series of OAZ knock-in experiments described here provide strong evidence that the presence of OAZ can perturb normal developmental timing and alter immature and mature ORN gene expression patterns. In this scenario, the transient OAZ expression during early differentiation contributes to a critical developmental switch during OE neurogenesis.

Consistent with the ability of OAZ to inhibit O/E-mediated transcription *in vitro*, ORNs that maintain *OAZ* expression *in vivo* are arrested at a differentiating stage precisely when the known targets of O/E (OMP, ORs and other olfactory transduction components) are first expressed. However, the re-expression of GAP43 when OAZ is reintroduced into mature cells (*O/E3*$^{OAZ\text{-}LNL/+}$*OMP*$^{CRE/+}$ mice) suggests that OAZ has additional functions beyond its action as an O/E inhibitor. A potential pathway involved in this transcriptional activation is the BMP-signaling pathway. *OAZ* is normally expressed at a stage when low-doses of BMP4 promotes survival of newly generated NCAM-positive immature cells in olfactory cultures (Shou et al., 2000). It would be interesting to determine whether BMP4 regulates GAP43 expression. Taken together, our experiments support a model in which OAZ may coordinately regulate immature and mature gene expression by integrating extrinsic microenvironmental cues (BMP-pathway) with an intrinsic transcriptional cascade (O/E pathway).

Involvement of *OAZ* in OR gene selection

The molecular mechanisms controlling OR gene choice and expression remains largely unresolved. While a specific genomic element, the "H region", is suggested to function as a global enhancer promoting OR expression (Lomvardas et al., 2006; Serizawa et al., 2003), the molecular interactions and proteins that participate in this complex process are unknown. These studies and related experiments on feedback mechanisms in OR gene choice suggest that the OR selection takes place within a defined time window during ORN development (Lewcock and Reed, 2003; Lewcock and Reed, 2004; Mombaerts, 2004). The expression of OAZ during this window and the phenotype observed in $O/E3^{OAZ/+}$ mice suggest that it may participate in OR selection. The increased number of immature M72-expressing cells in $O/E3^{OAZ/+}$ mice may derive from neuronal precursors that are arrested in development by sustained *OAZ* expression and accumulate multiple, activated OR genes in each cell. Unfortunately, the low level of reporter expression in these immature cells has precluded direct examination of this interesting question. Alternatively, maintained OAZ expression could promote differential selection of particular OR gene family members. The $O/E3^{OAZ/+}$ mice may also facilitate the study of OR selection by providing large numbers of genetically-tagged differentiating cells arrested in development.

ORNs in $O/E3^{OAZ/+}$ mice escape the gain-of-function phenotype at low frequency

The dramatic reduction of mature ORNs in $O/E3^{OAZ/+}$ mice is accompanied by a fraction of cells (~5% - "escapers") that mature and express OMP and AC3. Double-label experiments reveal that the escaper cells do not express the reporter-tagged *OE3-OAZ* allele. The arrest phenotype associated with the *OE3-OAZ* allele is dominant and individual cells that silence this allele epigenetically or by loss-of-heterozygosity (LOH) during mitotic recombination will have a distinct survival advantage. The inability of these escapers to converge to discrete glomeruli may reflect their abnormal developmental history, altered OR expression or the reduced number of cells of each OR type in the epithelium.

OAZ knock-in functions a dominant *O/E* suppressor

The *O*/*E* transcription factors are involved in many developmental processes (Corradi et al., 2003; Garel et al., 1999; Garel et al., 2002; Kieslinger et al., 2005; Lin and Grosschedl, 1995). The redundant expression of different *O*/*E* family members has limited our ability to study these processes by conventional gene-targeted inactivation. For example, disruption of *EBF1,* the founding member of this family, leads to profound developmental defects in B cells and striatum tissues that express only this member of the O/E family (Garel et al., 1999; Lin and Grosschedl, 1995), but its loss results in modest, if any, phenotype in the OE where it is highly expressed. Similarly, *O*/*E2* and *O*/*E3* knockout mice as well as *O*/*E2O*/*E3* double heterozygous mice displayed modest defects of ORN projection suggesting complex interactions and considerable functional redundancy with the additional *O*/*E* family members expressed in the OE (Wang et al., 2004). The ability of the OAZ protein to inhibit the function of all *O*/*E* family members *in vitro* (Tsai and Reed, 1997) and the expression of the *O*/*E3-OAZ* allele in all olfactory neuronal progenitors provides powerful tools to functionally disrupt all O/E function in this tissue. The abundant, persistent expression of the *O*/*E3* locus in mature olfactory neurons may make these cells particular susceptible to this dominant suppression.

Experimental Procedures

Mouse Genetics

The generation of OAZ^{lacZ} and *OAZ*-null mice, and their phenotype outside of the olfactory system are described elsewhere (Cheng and Reed, 2007; see supplemental methods). The *OAZ* knock-in was created from the *O*/*E3* knock-out targeting vector (Wang et al., 2004) and

modified by inserting the full-length *OAZ* cDNA 261 base pairs before the initiation codon for *O/E3*. The *OAZ* cDNA was followed by an *IRES-3NLS-YFP-pA* cassette and *LoxP-TK(Δ)-Neo-LoxP (LTNL)* cassette. The OR reporter mice, *OMP-taulacZ* and *OMP-CRE* mice were obtained from Dr. P. Mombaerts. The sequences of primers for genotyping each of the lines are available from the authors.

X-gal Staining, Immunolocalization and *in situ* Hybridization

The X-gal staining (Mombaerts et al., 1996) and immunohistochemistry was performed on PFA-fixed cryostat sections. The primary antibodies were: AC3 (rabbit, 1:1000; Santa Cruz Biotechnology), GAP43 (rabbit, 1:200, Chemicon), GFP (rabbit, 1:1000, Molecular Probes), LacZ (mouse, 1:500, Promega), O/E (rabbit, 1:1000), OMP (goat, 1: 3000; provided by Dr. F. Margolis), Tyrosine hydroxylase (rabbit, 1:500; Chemicon), NCAM (mouse, 1:1000; Sigma). Alexa 488- or Alexa 546-labled secondary antibodies were used at 1:1000 dilution. For double staining of X-gal and GFP, sections were stained with X-gal staining solution overnight, fixed with 4% PFA and then followed by normal antibody staining procedure using the anti-GFP antibody.

In situ hybridization was performed on PFA-fixed sections following a standard protocol (Wang et al., 2004). The probes were: I7 (NM_010983), M4 (NM_146937) and M72 (NM_030553) coding sequence, GAP43 (nucleotides 147 to 860 of NM_008083), NeuroD1 (nucleotides 640 to 1192 of BC018241), Evi3 (nucleotides 1 to 1172 of BC021376) and OMP (NM_011010) partial cDNA. Images were obtained with a Zeiss Axioplan microscope or a Zeiss LSM 510 confocal laser-scanning microscope.

BrdU Labeling and TUNEL Staining

Adult mice or pregnant females were injected intraperitoneally with BrdU (Sigma) 50μg/g body weight 30min before they were sacrificed. PFA-fixed sections were incubated with 3N HCl for 30min before immunostaining with anti-BrdU antibody (rat, 1:100; Abcam). To visualize, either an Alexa 546-labled secondary antibody or ABC kit (vector) and FAST DAB tablet sets (Sigma) were used. For double labeling of BrdU with anti-GFP antibody, sections were incubated with anti-GFP antibody first, then washed and fixed with 4% PFA before proceeding with the acid treatment. The secondary antibody incubations were performed simultaneously. TUNEL staining was performed using Apoptag® in situ apoptosis detection kits (Chemicon) according to the manufacturer's instruction.

Cell Counting in Epithelium and Statistics

OMP counting was performed on images taken at 20× magnification (4 images at matched locations for each animal, the total length of OE was approximately 5mm). The total number of BrdU, TUNEL and specific OR cells were counted under the microscope from overlapping 20× fields for the entire OE region on matched sections (4–5 sections for each animal, the total length of OE sampled was from 85mm to 160mm). OE length was determined by tracing the outline of the epithelium basal lamina using Axiovision® software. The data is represented as mean±s.d. and two-tailed Student's *t*-test was used for statistical analysis.

Supplementary Material

Refer to Web version on PubMed Central for supplementary material.

Acknowledgments

We thank Dr. P. Mombaerts for the OR-reporter mice, OMP-lacZ and OMP-CRE mice (Rockefeller University); Dr. F. Margolis for the OMP antibody (University of Maryland); Dr. S. Warming for *OAZ* cDNA (National Cancer

Institute). We thank members of the Reed lab and Dr. J. Nathans for helpful discussions. This work was supported by the NIDCD and the Howard Hughes Medical Institute.

References

Alcaraz WA, Gold DA, Raponi E, Gent PM, Concepcion D, Hamilton BA. Zfp423 controls proliferation and differentiation of neural precursors in cerebellar vermis formation. Proc Natl Acad Sci U S A. 2006

Bakalyar HA, Reed RR. Identification of a specialized adenylyl cyclase that may mediate odorant detection. Science 1990;250:1403–1406. [PubMed: 2255909]

Baker H, Cummings DM, Munger SD, Margolis JW, Franzen L, Reed RR, Margolis FL. Targeted deletion of a cyclic nucleotide-gated channel subunit (OCNC1): biochemical and morphological consequences in adult mice. J Neurosci 1999;19:9313–9321. [PubMed: 10531436]

Brunet LJ, Gold GH, Ngai J. General anosmia caused by a targeted disruption of the mouse olfactory cyclic nucleotide-gated cation channel. Neuron 1996;17:681–693. [PubMed: 8893025]

Calof AL, Chikaraishi DM. Analysis of neurogenesis in a mammalian neuroepithelium: proliferation and differentiation of an olfactory neuron precursor in vitro. Neuron 1989;3:115–127. [PubMed: 2482777]

Calof AL, Bonnin A, Crocker C, Kawauchi S, Murray RC, Shou J, Wu HH. Progenitor cells of the olfactory receptor neuron lineage. Microsc Res Tech 2002;58:176–188. [PubMed: 12203696]

Cau E, Casarosa S, Guillemot F. Mash1 and Ngn1 control distinct steps of determination and differentiation in the olfactory sensory neuron lineage. Development 2002;129:1871–1880. [PubMed: 11934853]

Cheng LE, Reed RR. The transcription factor Zfp423/OAZ is required for cerebellar dvelopment and CNS midline patterning. Dev Biol. 2007 in press.

Corradi A, Croci L, Broccoli V, Zecchini S, Previtali S, Wurst W, Amadio S, Maggi R, Quattrini A, Consalez GG. Hypogonadotropic hypogonadism and peripheral neuropathy in Ebf2-null mice. Development 2003;130:401–410. [PubMed: 12466206]

Dewulf N, Verschueren K, Lonnoy O, Moren A, Grimsby S, Vande Spiegle K, Miyazono K, Huylebroeck D, Ten Dijke P. Distinct spatial and temporal expression patterns of two type I receptors for bone morphogenetic proteins during mouse embryogenesis. Endocrinology 1995;136:2652–2663. [PubMed: 7750489]

Garel S, Marin F, Grosschedl R, Charnay P. Ebf1 controls early cell differentiation in the embryonic striatum. Development 1999;126:5285–5294. [PubMed: 10556054]

Garel S, Yun K, Grosschedl R, Rubenstein JL. The early topography of thalamocortical projections is shifted in Ebf1 and Dlx1/2 mutant mice. Development 2002;129:5621–5634. [PubMed: 12421703]

Hata A, Seoane J, Lagna G, Montalvo E, Hemmati-Brivanlou A, Massague J. OAZ uses distinct DNA- and protein-binding zinc fingers in separate BMP-Smad and Olf signaling pathways. Cell 2000;100:229–240. [PubMed: 10660046]

Hentges KE, Weiser KC, Schountz T, Woodward LS, Morse HC, Justice MJ. Evi3, a zinc-finger protein related to EBFAZ, regulates EBF activity in B-cell leukemia. Oncogene 2005;24:1220–1230. [PubMed: 15580294]

Hirata T, Nakazawa M, Yoshihara S, Miyachi H, Kitamura K, Yoshihara Y, Hibi M. Zinc-finger gene Fez in the olfactory sensory neurons regulates development of the olfactory bulb non-cell-autonomously. Development 2006;133:1433–1443. [PubMed: 16540508]

Jones DT, Reed RR. Golf: an olfactory neuron specific-G protein involved in odorant signal transduction. Science 1989;244:790–795. [PubMed: 2499043]

Kawauchi S, Beites CL, Crocker CE, Wu HH, Bonnin A, Murray R, Calof AL. Molecular signals regulating proliferation of stem and progenitor cells in mouse olfactory epithelium. Dev Neurosci 2004;26:166–180. [PubMed: 15711058]

Kawauchi S, Shou J, Santos R, Hebert JM, McConnell SK, Mason I, Calof AL. Fgf8 expression defines a morphogenetic center required for olfactory neurogenesis and nasal cavity development in the mouse. Development 2005;132:5211–5223. [PubMed: 16267092]

Kieslinger M, Folberth S, Dobreva G, Dorn T, Croci L, Erben R, Consalez GG, Grosschedl R. EBF2 regulates osteoblast-dependent differentiation of osteoclasts. Dev Cell 2005;9:757–767. [PubMed: 16326388]

Ku M, Howard S, Ni W, Lagna G, Hata A. OAZ Regulates Bone Morphogenetic Protein Signaling through Smad6 Activation. J Biol Chem 2006;281:5277–5287. [PubMed: 16373339]

Lewcock JW, Reed RR. Neuroscience. ORs rule the roost in the olfactory system. Science 2003;302:2078–2079. [PubMed: 14684811]

Lewcock JW, Reed RR. A feedback mechanism regulates monoallelic odorant receptor expression. Proc Natl Acad Sci U S A 2004;101:1069–1074. [PubMed: 14732684]

Li J, Ishii T, Feinstein P, Mombaerts P. Odorant receptor gene choice is reset by nuclear transfer from mouse olfactory sensory neurons. Nature 2004;428:393–399. [PubMed: 15042081]

Lin H, Grosschedl R. Failure of B-cell differentiation in mice lacking the transcription factor EBF. Nature 1995;376:263–267. [PubMed: 7542362]

Lomvardas S, Barnea G, Pisapia DJ, Mendelsohn M, Kirkland J, Axel R. Interchromosomal interactions and olfactory receptor choice. Cell 2006;126:403–413. [PubMed: 16873069]

Mombaerts P, Wang F, Dulac C, Chao SK, Nemes A, Mendelsohn M, Edmondson J, Axel R. Visualizing an olfactory sensory map. Cell 1996;87:675–686. [PubMed: 8929536]

Mombaerts P. Odorant receptor gene choice in olfactory sensory neurons: the one receptor-one neuron hypothesis revisited. Curr Opin Neurobiol 2004;14:31–36. [PubMed: 15018935]

Nicolay DJ, Doucette JR, Nazarali AJ. Transcriptional regulation of neurogenesis in the olfactory epithelium. Cell Mol Neurobiol 2006;26:801–819.

Serizawa S, Miyamichi K, Nakatani H, Suzuki M, Saito M, Yoshihara Y, Sakano H. Negative feedback regulation ensures the one receptor-one olfactory neuron rule in mouse. Science 2003;302:2088–2094. [PubMed: 14593185]

Shim S, Bae N, Han JK. Bone morphogenetic protein-4-induced activation of Xretpos is mediated by Smads and Olf-1/EBF associated zinc finger (OAZ). Nucleic Acids Res 2002;30:3107–3117. [PubMed: 12136093]

Shou J, Rim PC, Calof AL. BMPs inhibit neurogenesis by a mechanism involving degradation of a transcription factor. Nat Neurosci 1999;2:339–345. [PubMed: 10204540]

Shou J, Murray RC, Rim PC, Calof AL. Opposing effects of bone morphogenetic proteins on neuron production and survival in the olfactory receptor neuron lineage. Development 2000;127:5403–5413. [PubMed: 11076761]

Stryke D, Kawamoto M, Huang CC, Johns SJ, King LA, Harper CA, Meng EC, Lee RE, Yee A, L'Italien L, et al. BayGenomics: a resource of insertional mutations in mouse embryonic stem cells. Nucleic Acids Res 2003;31:278–281. [PubMed: 12520002]

Tsai RY, Reed RR. Cloning and functional characterization of Roaz, a zinc finger protein that interacts with O/E-1 to regulate gene expression: implications for olfactory neuronal development. J Neurosci 1997;17:4159–4169. [PubMed: 9151733]

Tsai RY, Reed RR. Identification of DNA recognition sequences and protein interaction domains of the multiple-Zn-finger protein Roaz. Mol Cell Biol 1998;18:6447–6456. [PubMed: 9774661]

Vassar R, Chao SK, Sitcheran R, Nunez JM, Vosshall LB, Axel R. Topographic organization of sensory projections to the olfactory bulb. Cell 1994;79:981–991. [PubMed: 8001145]

Verhaagen J, Greer CA, Margolis FL. B-50/GAP43 Gene Expression in the Rat Olfactory System During Postnatal Development and Aging. Eur J Neurosci 1990;2:397–407. [PubMed: 12106027]

Wang MM, Reed RR. Molecular cloning of the olfactory neuronal transcription factor Olf-1 by genetic selection in yeast. Nature 1993;364:121–126. [PubMed: 8321284]

Wang MM, Tsai RY, Schrader KA, Reed RR. Genes encoding components of the olfactory signal transduction cascade contain a DNA binding site that may direct neuronal expression. Mol Cell Biol 1993;13:5805–5813. [PubMed: 7689152]

Wang SS, Tsai RY, Reed RR. The characterization of the Olf-1/EBF-like HLH transcription factor family: implications in olfactory gene regulation and neuronal development. J Neurosci 1997;17:4149–4158. [PubMed: 9151732]

Wang SS, Lewcock JW, Feinstein P, Mombaerts P, Reed RR. Genetic disruptions of O/E2 and O/E3 genes reveal involvement in olfactory receptor neuron projection. Development 2004;131:1377–1388. [PubMed: 14993187]

Warming S, Liu P, Suzuki T, Akagi K, Lindtner S, Pavlakis GN, Jenkins NA, Copeland NG. Evi3, a common retroviral integration site in murine B-cell lymphoma, encodes an EBFAZ-related Kruppel-like zinc finger protein. Blood 2003;101:1934–1940. [PubMed: 12393497]

Warming S, Rachel RA, Jenkins NA, Copeland NG. Zfp423 is required for normal cerebellar development. Mol Cell Biol 2006;26:6913–6922. [PubMed: 16943432]

Wu HH, Ivkovic S, Murray RC, Jaramillo S, Lyons KM, Johnson JE, Calof AL. Autoregulation of neurogenesis by GDF11. Neuron 2003;37:197–207. [PubMed: 12546816]

Zhang D, Mehler MF, Song Q, Kessler JA. Development of bone morphogenetic protein receptors in the nervous system and possible roles in regulating trkC expression. J Neurosci 1998;18:3314–3326. [PubMed: 9547239]

Zheng C, Feinstein P, Bozza T, Rodriguez I, Mombaerts P. Peripheral olfactory projections are differentially affected in mice deficient in a cyclic nucleotide-gated channel subunit. Neuron 2000;26:81–91. [PubMed: 10798394]

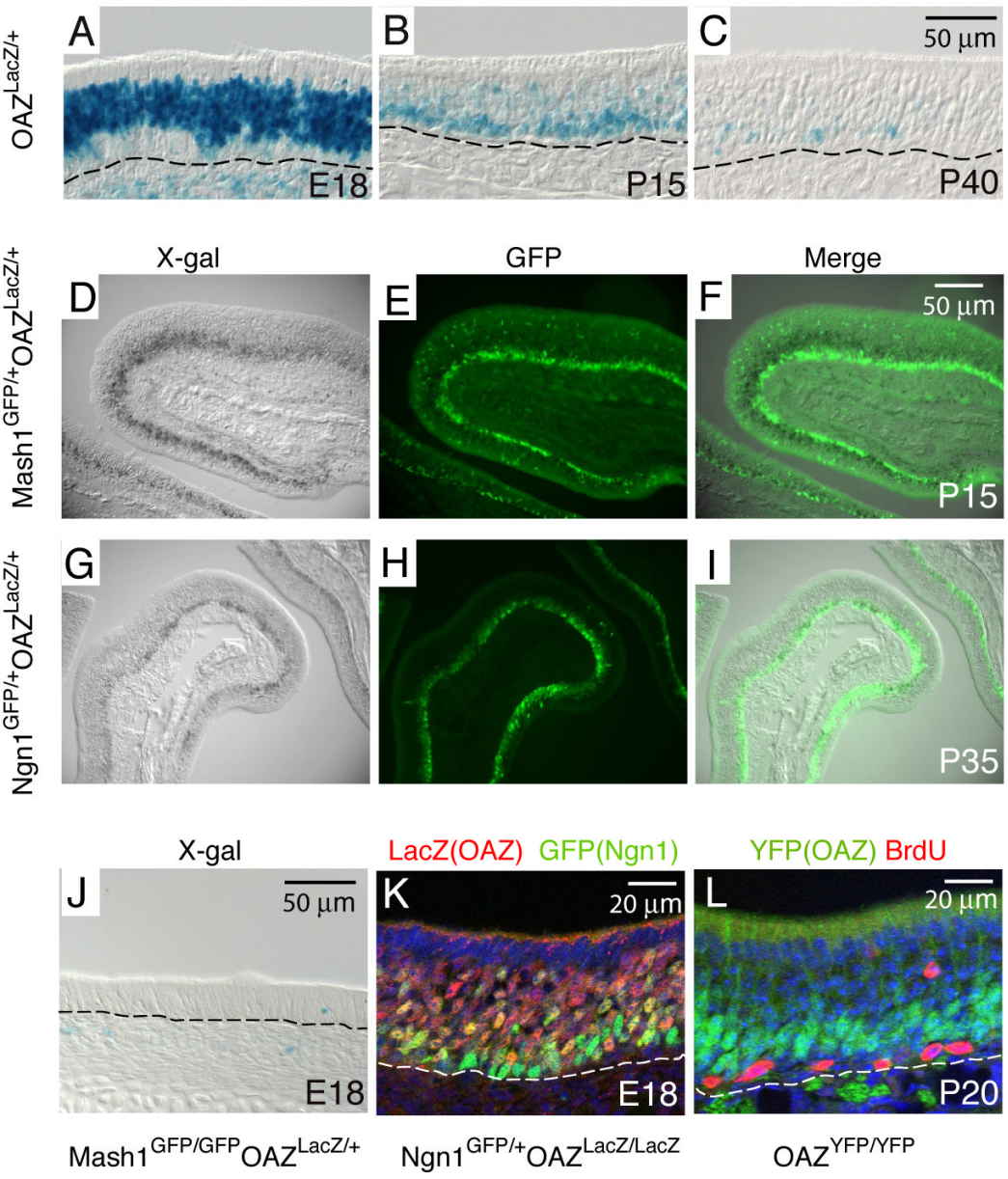

Figure 1. *OAZ* is expressed in newly differentiating ORNs

(A) In $OAZ^{lacZ/+}$ mice, X-gal positive cells are present in a broad region in the OE at E18. (B, C) At P15 and P40, X-gal positive cells become restricted to the basal OE. The basal lamina is indicated by dashed line. (D-F) OAZ is expressed downstream of *Mash1*. *OAZ*-expressing cells were identified by X-gal staining (D) and *Mash1*-expressing cells were identified with an anti-GFP antibody (E). In the merged picture (F), X-gal positive cells are located above GFP-positive cells. (G-I) In $OAZ^{lacZ/+}Ngn1^{GFP/+}$ mice, X-gal positive *OAZ*-expressing cells are in the same layer as GFP-positive *Ngn1*-expressing cells. (J) *OAZ*-expressing cells are absent in *Mash1*-null mice. (K) Colocalization of *OAZ* and *Ngn1* in the OE of $OAZ^{lacZ/lacZ}Ngn1^{GFP/+}$ mice. (L) *OAZ* is expressed in postmitotic cells in the OE. *OAZ*-expressing cells were identified in homozygous $OAZ^{YFP/YFP}$ mice (see figure 2) with an anti-GFP antibody (green) and proliferating cells were labeled with BrdU (red).

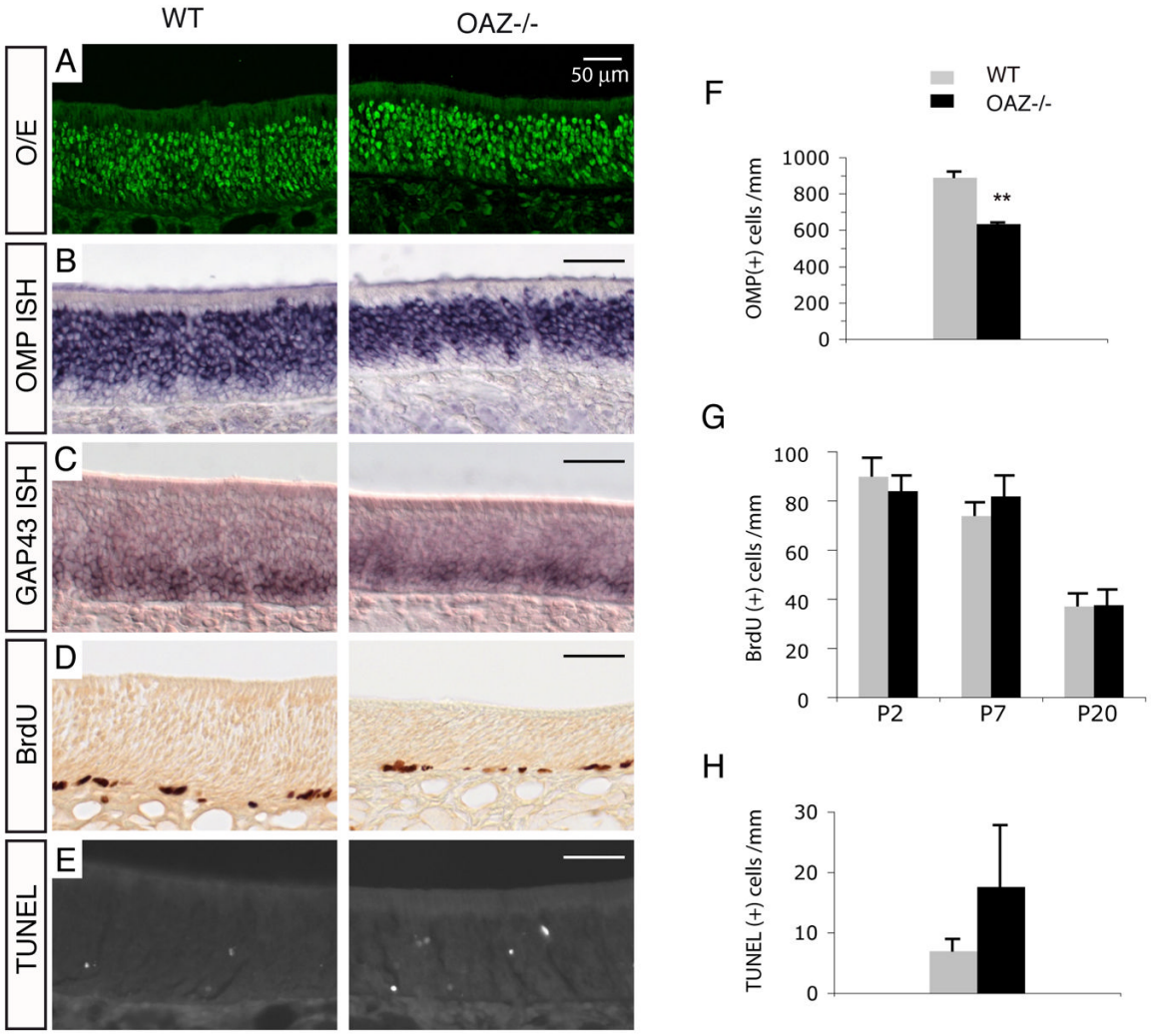

Figure 2. Characterization of OE in *OAZ*$^{-/-}$ mice

(A–E) O/E immunostaining, OMP and GAP43 *in situ* hybridization, BrdU labeling and TUNEL staining in wild-type and *OAZ*$^{-/-}$ mice. There is a reduction of mature cells and a two-fold increase of apoptotic cells in *OAZ*$^{-/-}$ mice. (F) Quantification of OMP-positive cells reveals a 30% reduction in *OAZ*$^{-/-}$ mice (wt, 890±30/mm; *OAZ*$^{-/-}$, 635±15/mm; n=3, $p<0.001$). (G) Quantification of BrdU-positive cells in the OE at P2, P7 and P20 (n=2 mice for each genotype at each age group). (H) Quantification of TUNEL-positive cells in the OE (wt, 7.0±1.9/mm, n=6; *OAZ*$^{-/-}$, 17.6±10/mm, n=5, $p<0.03$). Mice examined were from P20-P25 except that BrdU labeling was conducted at three ages.

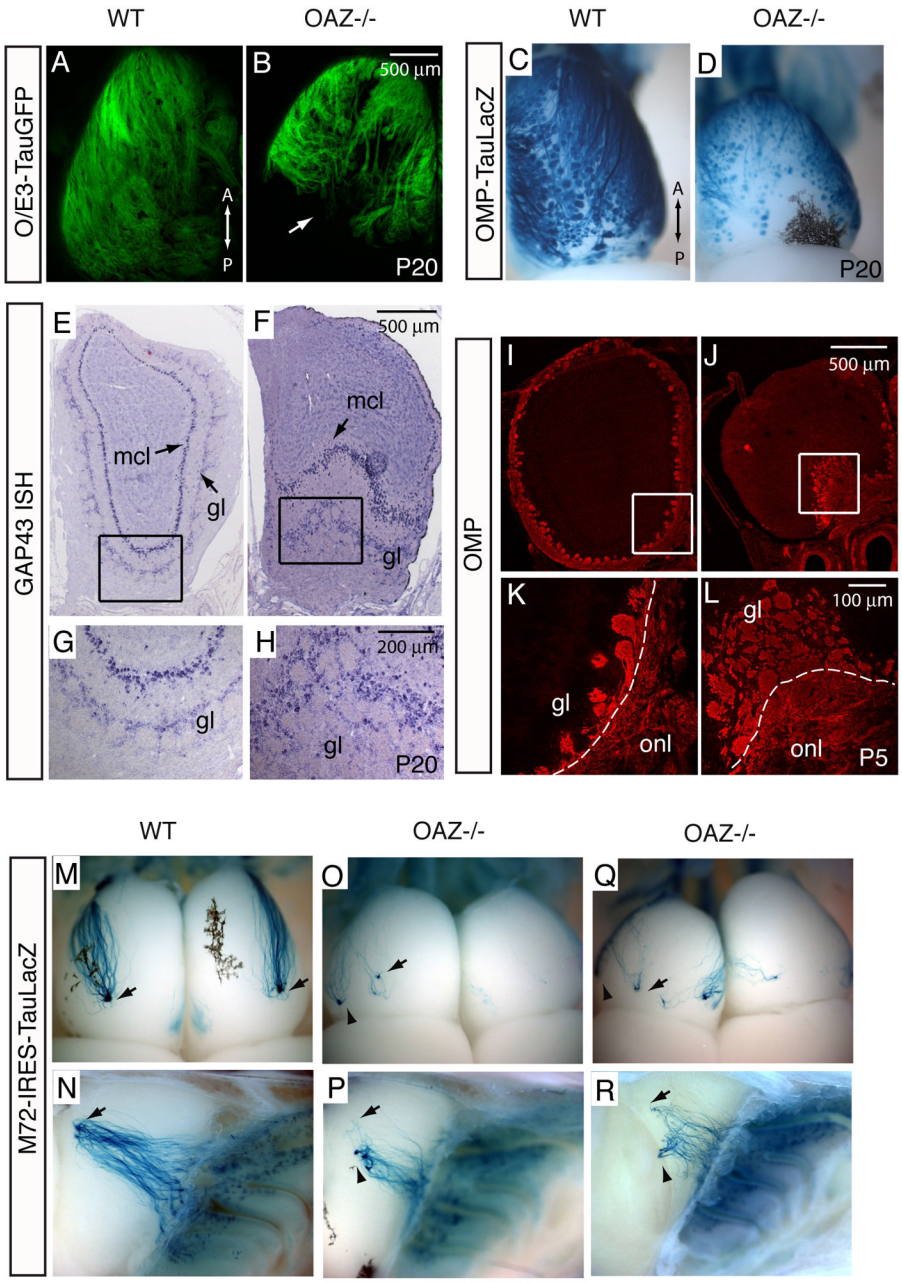

Figure 3. *OAZ*$^{-/-}$ mice exhibit ORN projection defects

(A–D) The ORN projection to the OB is visualized by *O/E3-tauGFP* reporter (A, B) and *OMP-taulacZ* reporter (C, D). In whole-mount dorsal view, ORN axons fail to innervate the caudal OB in *OAZ*$^{-/-}$ mice (n>6). (E, H) GAP43 *in situ* hybridization labels mitral cells and periglomerular cells in the OB. In *OAZ*$^{-/-}$ mice, the dorsal OB surface is devoid of glomeruli. The mitral cell layer (mcl) at the ventral OB is pushed inwardly by the abnormally accumulated glomeruli. (I–L) Labeling of olfactory axons with OMP antibody reveals tangled axons and disorganized glomeruli on the ventral surface in a P5 *OAZ*$^{-/-}$ mouse. (M–R) Poor convergence and a ventral shift of the M72 glomeruli in *OAZ*$^{-/-}$ mice. Projection of the M72-expressing axons is visualized by X-gal staining in *M72-IRES-taulacZ* reporter mice. As M72-expressing neurons converge to one lateral and one medial glomerulus in each bulb in control mice (arrows

in M, N), the M72 glomerulus in *OAZ*$^{-/-}$ mice is shifted ventrally (arrowheads in O-R, n=6) and a subset of axons miss their target. All reporter mice examined were from P20-P25.

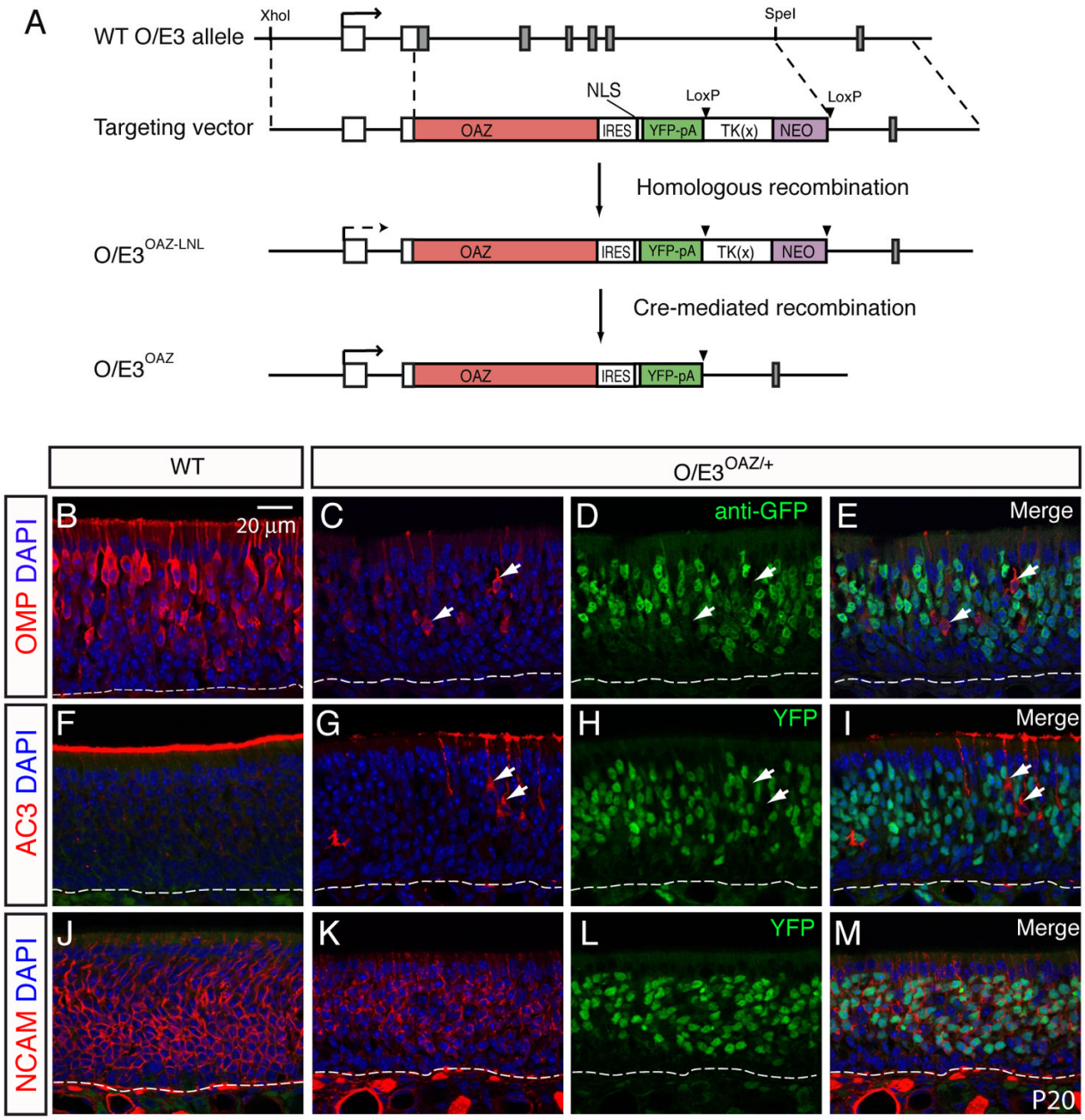

Figure 4. Sustained *OAZ* expression arrests ORN maturation

(A) Schematic representation of the *OAZ* knock-in strategy. Full length *OAZ* cDNA, followed by *IRES-3NLS-YFP-pA* and *LTNL* cassette was inserted in the 5′UTR of the *O/E3* gene, replacing the first five exons of *O/E3*. Transcription initiation sites are indicated by arrow. The *LTNL* cassette can be deleted by CRE-mediated recombination. (B-M) OMP, AC3 and NCAM staining in wild-type (B, F, J) and $O/E3^{OAZ/+}$ mice (C, G, K) at P20 revealed a dramatic reduction of mature cells in $O/E3^{OAZ/+}$ mice. The distribution of OAZ-expressing cells was visualized by either GFP antibody (D) or direct YFP fluorescence (H, L). The merged images (E, I, M) show that OAZ expression does not overlap with mature markers but overlaps with neuronal marker NCAM.

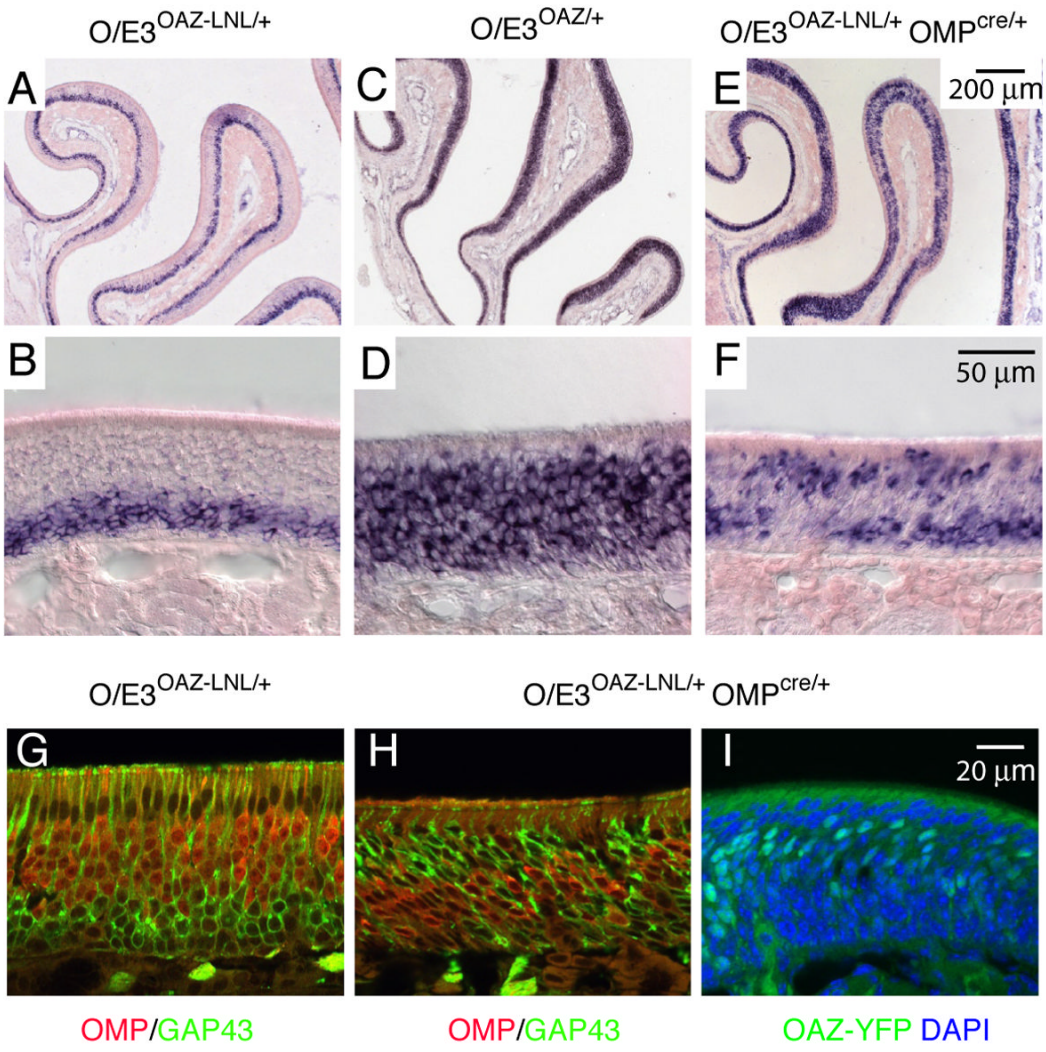

Figure 5. *OAZ* expression is sufficient for an immature phenotype

(A–D) GAP43 *in situ* hybridization demonstrates that the majority of cells in the epithelium are arrested at an immature stage in *O/E3*$^{OAZ/+}$ mice and the absolute number of GAP43-positive cells in the epithelium is increased. (E–F) In *O/E3*$^{OAZ\text{-}LNL/+}$*OMP*$^{CRE/+}$ mice, in which *OAZ-YFP* is selectively expressed in mature cells, a second population of GAP43-expressing cell is identified at the apical epithelium. (G, H) OMP/GAP43 double labeling in *O/E3*$^{OAZ\text{-}LNL/+}$*OMP*$^{CRE/+}$ mice shows that OMP and GAP43 are regulated in a reciprocal fashion by *OAZ*; in the apical GAP43-expressing cells, OMP expression is repressed. (I) *OAZ-YFP* reporter shows the reintroduction of *OAZ* expression (green) in mature cells in *O/E3*$^{OAZ\text{-}LNL/+}$*OMP*$^{CRE/+}$ mice. Mice examined were from P20-P25.

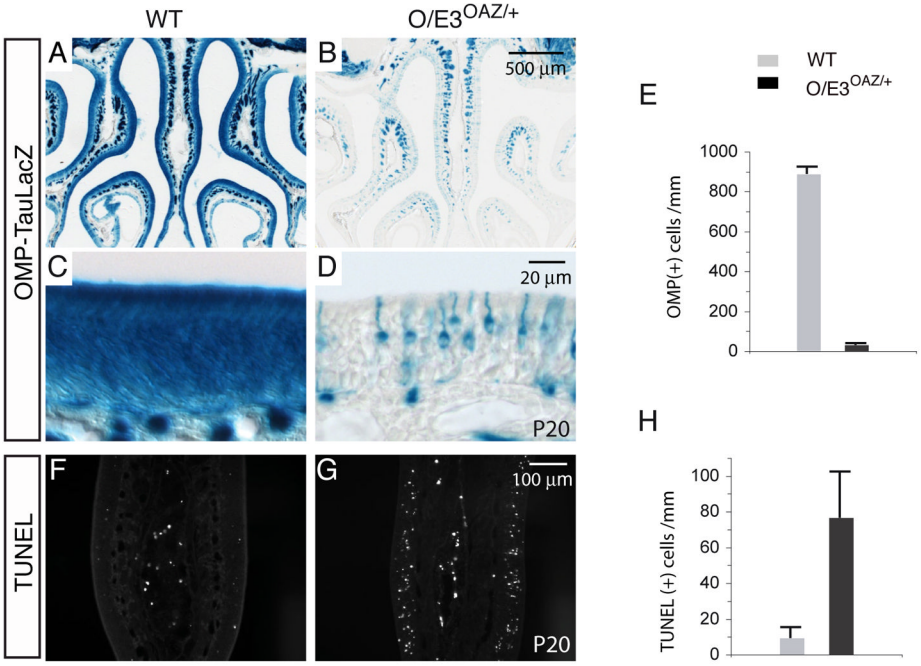

Figure 6. Defects of ORN maturation and increased apoptosis in *O/E3*$^{OAZ/+}$ mice

(A–D) X-gal staining of the OMP-taulacZ reporter confirms the reduction of mature cells in *O/E3*$^{OAZ/+}$ mice. (E) Quantification of OMP-positive cells in wild-type and *O/E3*$^{OAZ/+}$ mice (wt, 865±66/mm; *O/E3*$^{OAZ/+}$, 47±28/mm, n=3, P<0.001). (F, G) TUNEL staining shows a dramatic increase of apoptotic cells in the OE of *O/E3*$^{OAZ/+}$ mice. (H) Quantification of TUNEL-positive cells (wt, 9.4±5.4/mm, n=3; *O/E3*$^{OAZ/+}$, 76.5±25.2/mm, n=3, P<0.01).

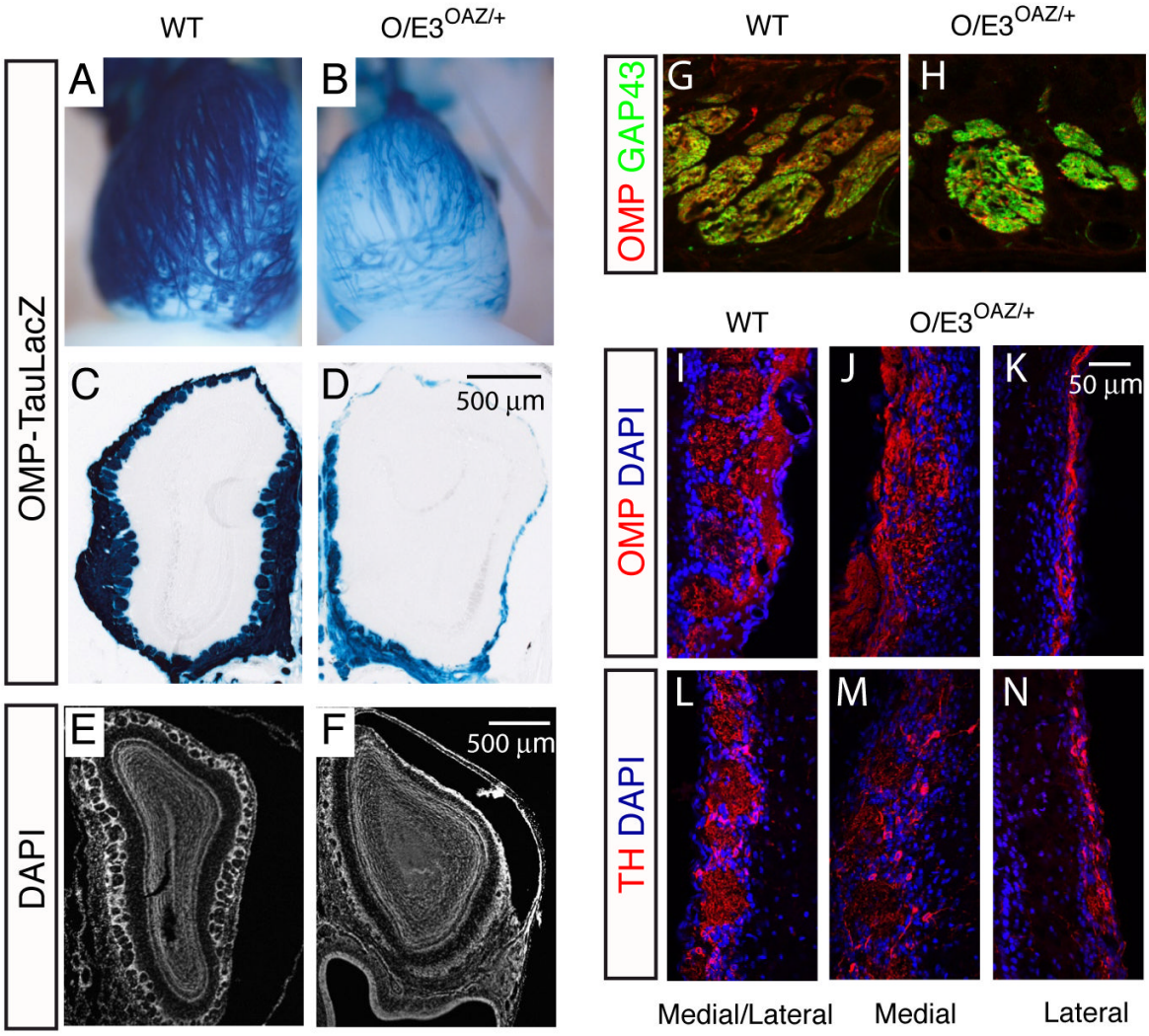

Figure 7. Defects in the ORN projection in *O/E3*$^{OAZ/+}$ mice

(A, B) Whole-mount X-gal staining reveals that the dorsal OB is largely devoid of glomeruli. (C–F) Coronal sections through the OB confirm the reduced ONL and absence of dorsal glomeruli in *O/E3*$^{OAZ/+}$ mice. (G, H) OMP/GAP43 double-labeling of axon bundles. In *O/E3*$^{OAZ/+}$ mice, axon bundles are GAP43-positive and a small fraction of axons are OMP-positive, suggesting that GAP43-expressing immature cells initiate their axonal growth in *O/E3*$^{OAZ/+}$ mice. (I–K) OMP staining demonstrates that the medial OB surface contains OMP-positive olfactory axons and disorganized glomerular structures, while the lateral surface is covered by thin ONL. (L–N) The expression of tyrosine hydroxylase in periglomerular interneurons is greatly reduced at the lateral OB in *O/E3*$^{OAZ/+}$ mice. Mice examined were from P20-P25.

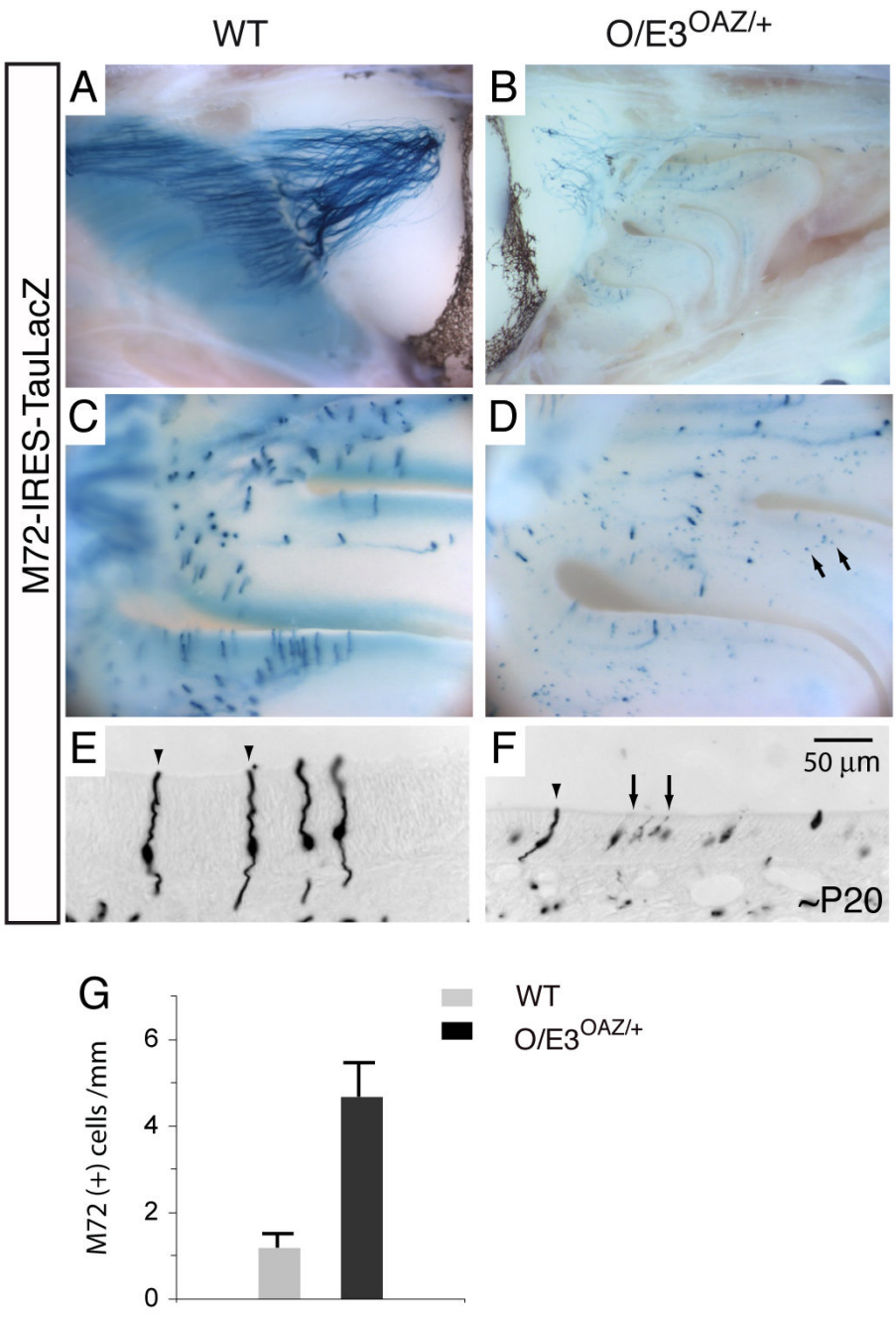

Figure 8. Sustained *OAZ* expression alters OR gene expression

(A, B) Whole-mount X-gal staining of *M72-IRES-taulacZ* reporter. The axons from M72-expressing cells in *O/E3*$^{OAZ/+}$ mice do not converge, but project along the dorsal to ventral surface of the OB. (C, D) In the *O/E3*$^{OAZ/+}$ epithelium, the strongly stained axon-projecting M72-expressing cells are accompanied by a large number of weakly stained non-projecting cells (arrows). (E, F) In coronal sections, the weakly stained cells (arrows) display short dendrites and no obvious axon extensions. The signal below the basal lamina reflects individual axons stained in cross sections. (G) Quantification of M72-expressing cells in control and *O/E3*$^{OAZ/+}$ mice (wt, 1.2±0.3/mm, n=3; *O/E3*$^{OAZ/+}$, 4.7±0.7/mm, n=3, P<0.002). Mice examined were from P20-P25.